

Nucleation and high-density packing of 360° domain walls on planar ferromagnetic nanowires by using circular magnetic fields

F. I. Kaya,¹ A. Sarella,¹ D. Wang,² M. Tuominen,² and K. E. Aidala^{1, a)}

¹⁾*Department of Physics, Mount Holyoke College, South Hadley, MA, 01075, USA*

²⁾*Department of Physics, University of Massachusetts, Amherst, MA, 01003, USA*

(Dated: 31 October 2015)

We propose a mechanism for nucleation and high-density packing of 360° domain walls (DWs) on planar ferromagnetic nanowires, of 100 nm width, by using circular magnetic fields. The extent of the stray field from a 360° DW is limited in comparison to 180° DWs, which allows them to be packed more densely than 180° DWs in a potential data storage device. We use micromagnetic simulations to demonstrate high-density packing of 360° DWs, using a series of rectangular $16 \times 16 \text{ nm}^2$ notches to act as local pinning sites on the nanowires. For these notches, the minimum spacing between the DWs is 240 nm, corresponding to a 360° DW packing density of 4 DWs per micron. Understanding the topological properties of the 360° DWs allows us to understand their formation and annihilation in the proposed geometry. Adjacent 360° DWs have opposite circulation, and closer spacing result in the adjacent walls breaking into 180° DWs and annihilating.

Keywords: 360° , domain wall, nucleation, nanowire, ferromagnetic, circular magnetic field, manipulation, packing, density, high-density, notches, rectangular

Manipulating magnetic domain walls (DWs) in patterned ferromagnetic nanostructures and understanding their behavior are necessary to achieve proposed logic¹ and data storage devices.² Racetrack memory proposes the use of current driven transverse 180° DWs, which interact over a range of about $2.5 \text{ }\mu\text{m}$.^{3,4} In contrast, 360° DWs form an almost closed flux magnetic state, substantially reducing the interaction between neighboring DWs. For this reason, 360° DWs have been proposed to serve as bits for data storage in a magnetic racetrack device.⁵ A 360° DW can be viewed as consisting of two 180° DWs, and whether bringing together two transverse 180° DWs results in annihilation or a 360° DW depends on the topological edge charges of the 180° DWs.^{6,7} Current driven motion of 360° DWs is predicted to be different from 180° DWs,^{8,9} but experimental confirmation has been challenging. Reliable nucleation and manipulation mechanisms are needed to study the properties of the 360° DWs and to develop devices. Most proposals involve an injection pad with a rotating in-plane field,^{8,10–12} with the exception of Gonzalez Oyarce et al.¹³ Here, we propose a versatile technique to controllably nucleate 360° DWs at arbitrary locations using a circular field centered in close proximity to a planar nanowire, allowing for the study of 360° DWs in a wire and the potential to develop novel storage devices.

We perform micromagnetic simulations using the OOMMF¹⁴ package to iteratively solve the Landau-Lifshitz-Gilbert equation. The nanowire dimensions used in the simulations are $10000 \times 100 \text{ nm}^2$ and the material parameters are for permalloy: $M_s = 8 \times 10^5 \text{ A/m}$, $A = 1.3 \times 10^{-11} \text{ J/m}$. The cell size is 4 nm along the

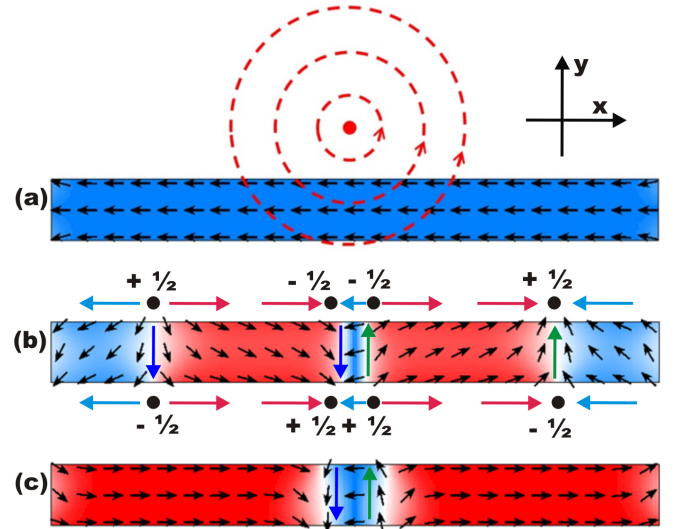


FIG. 1. (a) Initialization of the nanowire and top-down view of the circular field. (b) Snapshot showing the nucleation of a 360° DW and two 180° DWs. (c) Relaxed state of a single 360° DW. The color scale in (b) and (c) indicate the orientation of the moments along the x -axis: Red points to the right, blue to the left. Green and blue arrows help identify the topological winding of the DWs.

three axes, there is no crystalline anisotropy, the damping parameter is 0.5, and simulations are run at 0 K. The magnetization state evolves until structures reach an equilibrium state where $\frac{dM}{dt} < 0.1 \text{ deg/ns}$.

Figure 1a shows the mechanism for nucleating a 360° DW. We initialize the nanowire by magnetizing it along the negative x -axis with a large in-plane magnetic field of 160 mT or higher. We apply a circular field, simulated as if from a current in an infinitely long wire that flows into

^{a)}Electronic mail: kaidala@mtholyoke.edu.

the page, which produces a field that decreases as $1/r$, where r is the distance from the center of the field. A current of 21 mA, which is located at a distance of $r = 48$ nm from the nanowire along the positive y -axis, corresponds to a field of 87.5 mT at the top edge of the wire. The circular field exerts a torque on the magnetic moments, whereby it nucleates a 360° DW in the nanowire directly below the center of the circular field (Fig. 1b). Two 180° DWs are created on either side of the 360° DW. The moments directly below the center of the magnetic field experience the smallest torque (theoretically zero in a perfect structure at zero temperature, since they are aligned opposite to the applied field), while the other moments feel stronger torques to align with the field. Such circular fields can be experimentally implemented via the tip of an Atomic Force Microscope (AFM),^{15,16} which can be positioned at arbitrary locations to follow the pattern of fields described in this paper. For a scalable device, the procedure would presumably be realized by fabricating wires above each notch and by passing current through those wires perpendicular to the plane of the nanowire.

The simultaneous nucleation of two 180° DWs on either side of the 360° DW is a topological consequence, and is described in Bickel et al. for rings.¹⁷ We characterize the 180° DWs as “up” or “down” as conveniently revealed by whether the moments at their center are pointing in positive or negative y , indicated by the green or blue arrows in Figure 1b. We use the same terminology for the 360° DWs, which can be “up-down” or “down-up” depending on the constituent 180° DWs (read from left to right). Figure 1b is a snapshot in time during the nucleation of a 360° DW, while the circular field is still applied. The half integer winding numbers of the topological edge charges^{6,7} are indicated as well. At the nucleation of the 360° DW, two topological defects with charge $-1/2$ are created on the top edge of the nanowire (Fig. 1b), and two $+1/2$ charges are created at the bottom. Two switched (red) domains appear on either side of the 360° DW, aligning with the applied field. Two 180° DWs must also be created (at the farther edge of the switched domain), and these must carry the opposite topological charges, $+1/2$ on the top and $-1/2$ on the bottom. The total winding number of the wire is zero, as required.

Given our CCW field and the resulting down-up 360° DW, the 180° DW that emerges to the right of the 360° DW is an up 180° DW, while the one to the left is a down 180° DW. If a down 180° DW joins with another down 180° DW, the topological edge charges sum up to zero on the top and the bottom, hence the DWs annihilate. Similarly, the joining of two up 180° DWs results in annihilation.

When the applied circular field is removed, the wire in Figure 1 relaxes to the state shown in Figure 1c. The 180° DWs are pushed to the side until they encounter the end of the wire and annihilate. This is generally not the case for longer wires in which the 360° DW slides towards one of the 180° DWs and eventually annihilates

into a single 180° DW as a result of the summation of the topological charges.

In order to pin 360° DWs on the nanowire, a series of rectangular notches of 16×16 nm² are introduced with an inter-notch distance of 280 nm (Fig. 2). The length (y -axis) of the DW is reduced at the notches, thereby reducing the energy of the DWs and facilitating pinning at the notches. Figure 2 demonstrates the sequence of steps required to generate a series of 360° DWs with opposite circulation at adjacent notches. Once the nanowire is saturated along the negative x -axis as shown in Figure 2a, the first CW 360° DW is nucleated at notch **I** by passing a current of 21 mA vertically above the notch. As a result, an up 180° DW pins at notch **II**, while the down 180° DW slides to the end of the wire and annihilates due to the field gradient at the edge. The second 360° DW at notch **III** is injected by following the same procedure. The simultaneously nucleated down 180° DW to the left pairs with the up 180° DW that was earlier nucleated and pinned at notch **II**, forming a CCW 360° DW as shown in Figure 2c. Similarly, the circular field is positioned at notch **V** to nucleate the CW 360° DW at **V** and form the CCW 360° DW at **IV**. The magnetization circulation of the packed domain walls at notches **I** to **V** alternate between CW and CCW circulation, as shown in Figure 2d.

We have successfully simulated packing of 360° DWs at adjacent notches with 260 nm and 240 nm inter-notch distances. As the notches are spaced more closely, the field strength is higher at notches adjacent to where the 360° DW is nucleated. The 180° DWs do not pin at the adjacent notch but are instead pinned two notches away. The second nucleated 360° DW must also be formed an additional notch away. It is straightforward to push these nucleated DWs to neighboring notches, by effectively unravelling the 360° into two 180° DWs with the correct strength field, and then pushing the 180° DWs with an appropriate strength field.

The packing collapses if the distance between adjacent notches is ≤ 220 nm. Figure 3 shows why the previously described procedure fails when the notches are too close together, at 220 nm. We first nucleate the down-up 360° DW at **I**, creating an up 180° DW at **II**. We nucleate the second 360° DW at notch **IV**, as the 180° DW at notch **II** is too close to notch **III** and prevents the nucleation of a down 180° DW to the left of notch **III**. We instead nucleate the down-up 360° DW at notch **IV**, and see that the down 180° DW moves to notch **III** and the 180° DWs at **II** and **III** are interacting, shown in Figure 3a. Figure 3b shows that by applying a CCW field at notch **III**, we can temporarily form a tight 360° DW pinned at notch **III**. However, once the field is removed (Fig. 3c), the 360° DWs at notch **III** and **IV** annihilate one another due to their topological charges. Effectively, the two down constituent 180° DWs are adjacent, attract each other, and annihilate. The two up 180° DWs remain at notches **III** and **IV**. Therefore, a distance of ≤ 220 nm between notches prevents packing of 360° DWs

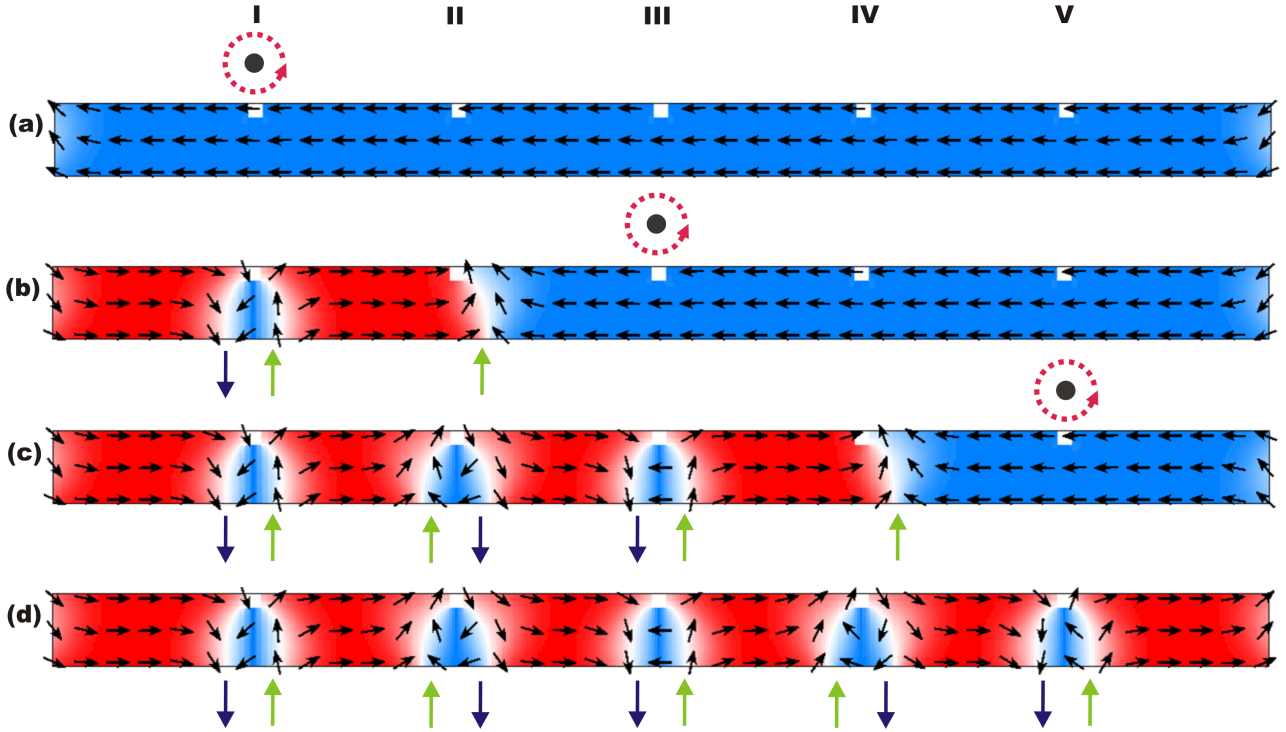


FIG. 2. The sequence of steps for packing 360° DWs of opposite circulation at adjacent notches. Red dotted lines indicate the center of the CCW circular field. (a) Initialization. (b) Resulting state after applying 21 mA above notch **I**. (c) Resulting state after applying 21 mA above notch **III**, creating a second 360° DW directly below, and two 180° DWs, one of which joins the 180° DW at notch **II** to form a 360° DW. (d) Resulting state after applying 21 mA above notch **V**.

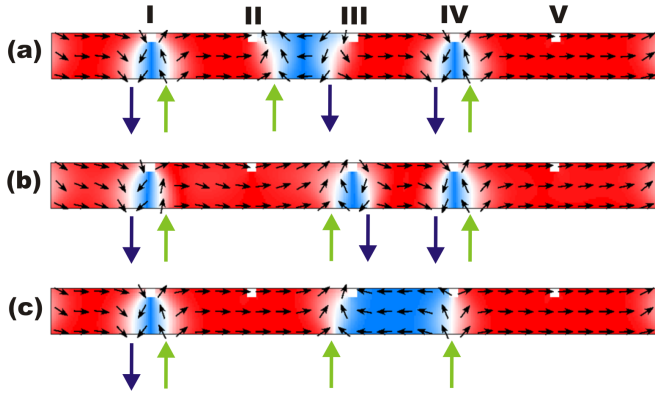


FIG. 3. Failure mechanism when packing opposite circulation 360° DWs at the inter-notch distance of 220 nm. (a) 360° DWs are formed at notches **I** and **IV**. The 180° DWs interact but do not come together at a single notch. (b) Temporarily applying a CCW field above notch **II** pushes the two 180° DWs into a tight 360° DW at notch **III**. (c) When the field is removed, the constituent down DWs are sufficiently close to interact and annihilate, leaving the two up DWs at their respective notches.

at adjacent notches on a nanowire, using this technique and geometry.

The minimum spacing between 360° DWs is deter-

mined in part by the notch size and shape. Deeper notches allow closer packing but require stronger fields to de-pin the DWs. We have succeeded in simulating a dense packing of 360° DWs at adjacent notches with 220 nm spacing by using $16 \times 32 \text{ nm}^2$ rectangular notches. The procedure in this case differs slightly due to the stronger pinning of 180° and 360° DWs at deeper notches. Additionally, if we control the topology of the adjacent 360° DWs so that they are all of the same circulation, the failure mechanism changes and we can pack the 360° DWs more densely. This can be accomplished by annihilating the DW with the circulation that we do not want by using a strong local field above that DW. For example, a strong enough (85 mA) CCW field at notch **I** in Figure 3a annihilates the 360° DW pinned at **I**. We can then shift the other 360° DWs by unravelling them into two 180° DWs and pushing the 180° DWs. For $16 \times 64 \text{ nm}^2$ rectangular notches, we can successfully pack 360° DWs with the opposite circulation at 180 nm spacing between the notches. More work remains to be done to better understand the effects of the geometry of the notches and the circulation of adjacent 360° DWs and their effects on the packing density.¹⁸

While these notched wires allow us to study the behavior of 360° DWs, and using the tip of an AFM to manipulate the DWs provides flexibility in our experiments, a realistic device would have prefabricated wires

positioned above each notch where we center the circular field in our simulations. The presence or absence of the 360° DW could be used as the bit, or possibly the circulation of the 360° DW. Geometry would be optimized to reduce the current density and power consumption while maintaining a close packing density. The read-out might be similar to racetrack memory,^{3,4} requiring a spin-polarized current to move the 360° DWs. Generally, there will be a trade-off between strong pinning providing closer packing, and weak pinning requiring smaller fields and current to move the DWs.

In summary, we propose a mechanism to nucleate 360° DWs at arbitrary locations determined by notches along an in-plane ferromagnetic nanowire. A circular field that decreases as $1/r$ and is centered directly above a notch along the y-axis will nucleate one 360° DW and two 180° DWs at that notch. Careful consideration of the series of circular fields allows us to nucleate 360° DWs with opposite circulation at adjacent notches as close as 240 nm, providing a packing density of about four DWs per micron in the permalloy nanowire simulated with $16 \times 16 \text{ nm}^2$ rectangular notches.

The authors acknowledged the support by NSF grants No. DMR 1208042 and 1207924. Simulations were performed with the computing facilities provided by the Center for Nanoscale Systems (CNS) at Harvard University (NSF award ECS-0335765), a member of the National Nanotechnology Infrastructure Network (NNIN).

¹G. Hrkac, J. Dean, and D. A. Allwood, *Philos. Trans. R. Soc. A* **369**, 3214–3228 (2011).

- ²S. S. P. Parkin, M. Haysahi, and L. Thomas, *Science* **320**, 190 (2008).
- ³M. Haysahi, L. Thomas, R. Moriya, C. Rettner, and S. Parkin, *Science* **320** (2008).
- ⁴L. Thomas, M. Hayashi, R. Moriya, C. Rettner, and S. Parkin, *Nat. Commun.* **3**, 810 (2012).
- ⁵A. L. G. Oyarce, Y. Nakatani, and C. H. W. Barnes, *Phys. Rev. B* **87**, 214403 (2013).
- ⁶A. Pushp, T. Phung, C. Rettner, B. P. Hughes, S.-H. Yang, L. Thomas, and S. S. P. Parkin, *Nature Phys.* **9**, 505 (2013).
- ⁷A. Kunz, *Appl. Phys. Lett.* **94**, 132502 (2009).
- ⁸M. Diegel and E. Mattheis, R. Halder, *IEEE Trans. Magn.* **40**, 2655–2657 (2004).
- ⁹M. D. Mascaro and C. A. Ross, *Phys. Rev. B* **82**, 214411 (2010).
- ¹⁰Y. Jang, S. R. Bowden, M. Mascaro, J. Unguris, and C. A. Ross, *Appl. Phys. Lett.* **100**, 062407 (2012).
- ¹¹L. D. Geng and Y. M. Jin, *J. Appl. Phys.* **112**, 083903 (2012).
- ¹²T.-C. Chen, C.-Y. Kuo, A. K. Mishra, B. Das, and J.-C. Wu, *Phys. B Condens. Matter* **476**, 1 (2015).
- ¹³A. L. Gonzalez Oyarce, J. Llandro, and C. H. W. Barnes, *Appl. Phys. Lett.* **103**, 222404 (2013).
- ¹⁴M. J. Donahue and D. G. Porter, *OOMMF user's Guide, Version 1.0*, Interagency Report NISTIR 6376 (National Institute of Standards and Technology). (1999).
- ¹⁵A. Goldman, A. S. Licht, Y. Sun, Y. Li, N. R. Pradhan, T. Yang, M. T. Tuominen, and K. E. Aidala, *J. Appl. Phys.* **111**, 07D113 (2012).
- ¹⁶T. Yang, N. R. Pradhan, A. Goldman, A. S. Licht, Y. Li, M. Kemei, M. T. Tuominen, and K. E. Aidala, *Appl. Phys. Lett.* **98**, 242505 (2011).
- ¹⁷J. E. Bickel, S. A. Smith, and K. E. Aidala, *J. Appl. Phys.* **115**, 17D135 (2014).
- ¹⁸F. I. Kaya, A. Sarella, K. E. Aidala, D. Wang, and M. Tuominen, (In preparation).